

## ARTICLE

# Overexpression of factor VIII after AAV delivery is transiently associated with cellular stress in hemophilia A mice

Amy M Lange<sup>1,2</sup>, Ekaterina S Altynova<sup>2</sup>, Giang N Nguyen<sup>1</sup> and Denise E Sabatino<sup>1,3</sup>

Factor VIII (FVIII) is a large glycoprotein that is challenging to express both *in vitro* and *in vivo*. Several studies suggest that high levels of FVIII expression can lead to cellular stress. After gene transfer, transgene expression is restricted to a subset of cells and the increased FVIII load per cell may impact activation of the unfolded protein response. We sought to determine whether increased FVIII expression in mice after adeno-associated viral liver gene transfer would affect the unfolded protein response and/or immune response to the transgene. The FVIII gene was delivered as B-domain deleted single chain or two chain (light and heavy chains) at a range of doses in hemophilia A mice. A correlation between FVIII expression and anti-FVIII antibody titers was observed. Analysis of key components of the unfolded protein response, binding immunoglobulin protein (BiP), and C/EBP homologous protein (CHOP), showed transient unfolded protein response activation in the single chain treated group expressing >200% of FVIII but not after two chain delivery. These studies suggest that supraphysiological single chain FVIII expression may increase the likelihood of a cellular stress response but does not alter liver function. These data are in agreement with the observed long-term expression of FVIII at therapeutic levels after adeno-associated viral delivery in hemophilia A dogs without evidence of cellular toxicity.

*Molecular Therapy — Methods & Clinical Development* (2016) **3**, 16064; doi:10.1038/mtm.2016.64; published online 28 September 2016

## INTRODUCTION

Factor VIII (FVIII) is a large glycoprotein that has a critical role in blood coagulation. Deficiencies of the clotting FVIII protein cause the X-linked bleeding disorder hemophilia A (HA) that affects 1 in 5,000 males in the population.<sup>1</sup> Hemophilia patients have frequent spontaneous bleeding episodes into the soft tissues and joints that contribute to the morbidity associated with the disease while intracranial bleeds can be fatal. The current treatment for hemophilia is protein replacement therapy using recombinant or plasma derived coagulation factor that requires frequent administration due to the short half-life of the protein. The development of gene-based therapeutic approaches has led to Phase 1 clinical trials for adeno-associated viral (AAV) delivery of factor IX for hemophilia B that have shown promising results with long term therapeutic levels of FIX expression that has alleviated the need for exogenous protein treatment in some patients.<sup>2,3</sup> While HA is more common in the population, the development of AAV delivery approaches for FVIII has additional challenges including the large size of the FVIII cDNA and the inefficient secretion of the protein.<sup>4</sup> Ongoing preclinical studies of liver-directed AAV-mediated delivery of FVIII have demonstrated therapeutic levels of FVIII in HA mice, HA dogs and nonhuman primates.<sup>5–9</sup>

FVIII is synthesized as a large precursor molecule (2,332 amino acids) with a domain structure consisting of A1-A2-B-A3-C1-C2 domains with the B domain that is dispensable for FVIII function.<sup>10</sup>

During intracellular processing, the FVIII translation product is translocated to the lumen of the endoplasmic reticulum (ER) where N-linked glycosylation occurs and FVIII is folded into a tertiary structure. FVIII may interact with chaperones (calnexin and calreticulin) that interact with the LMAN1/MCFD2 protein chaperone complex for transit to the Golgi.<sup>11</sup> Alternatively, misfolded protein may interact with the 78 kDa glucose-regulated protein (GRP78) also known as binding immunoglobulin protein (BiP) that serves as a quality control system for further secretion and some FVIII may be degraded by the 26S proteasome through ER-associated degradation.<sup>12,13</sup> Under conditions of cellular stress that cause protein misfolding, BiP activates a cascade of signals that initiate the unfolded protein response (UPR). While the UPR assists the cell to adapt and survive ER stress, prolonged ER stress causes pathological responses including inflammation and apoptosis.<sup>14</sup> After transit to the Golgi, FVIII undergoes additional processing and the mature FVIII is secreted into the circulation as a heterodimer.<sup>13,15</sup>

For many years it has been evident that it is challenging to express recombinant FVIII *in vitro* and *in vivo*. In recombinant production systems, low level FVIII expression is observed compared with other proteins of similar size such as factor V.<sup>11</sup> It has been challenging to express FVIII *in vitro* possibly due to inefficient mRNA translation, inefficient transport of FVIII from the ER to the Golgi or poor stability in the absence of vWF. The use of a B-domain deleted form of FVIII (FVIII-BDD) results in increased secretion of FVIII. *In vitro* studies in

<sup>1</sup>The Raymond G. Perelman Center for Cellular and Molecular Therapeutics, The Children's Hospital of Philadelphia, Philadelphia, Pennsylvania, USA; <sup>2</sup>Department of Genetics, Perelman School of Medicine, University of Pennsylvania, Philadelphia, Pennsylvania, USA; <sup>3</sup>Department of Pediatrics, Division of Hematology, Perelman School of Medicine, University of Pennsylvania, Philadelphia, Pennsylvania, USA. Correspondence: DE Sabatino (dsabatino@mail.med.upenn.edu)

Received 10 May 2016; accepted 2 August 2016

Chinese hamster ovary (CHO)<sup>16</sup> or baby hamster kidney cells<sup>17</sup> have demonstrated that misfolded FVIII in the ER leads to activation of the UPR resulting in FVIII degradation or apoptosis of the cell.

While there has been significant effort to understand the synthesis of FVIII *in vitro*, less is known about the implications of FVIII overexpression *in vivo*. In the setting of gene-based delivery approaches that target the liver, the FVIII expression is restricted to only a portion of the hepatocytes. High-level FVIII expression in a subset of cells may result in a large protein load per cell that could induce a cellular stress response that may impact the safety and efficacy of the approach. After hydrodynamic delivery of a plasmid expressing human FVIII (hFVIII) in wild type mice, ER stress was observed 24 hours after plasmid delivery.<sup>16</sup> In the setting of gene transfer using a plasmid based delivery approach of FVIII by a *piggyBac* transposon, cellular stress was not observed after 16 weeks post gene delivery.<sup>18</sup> The UPR after AAV mediated gene delivery of FVIII has not been evaluated.

Our objective was to characterize the cellular synthesis of FVIII *in vivo* and determine if the level of FVIII expression impacts efficacy and safety of gene delivery approaches. We have had a longstanding interest in canine FVIII (cFVIII) and our extensive preclinical studies of AAV-mediated gene transfer of cFVIII in the HA dog provide a unique opportunity to compare the mouse and dog studies.<sup>5</sup> After AAV-cFVIII delivery using a single chain (SC) or two-chain (TC) delivery approach, long-term dose dependent expression of therapeutic levels of FVIII were observed in both HA mice and dogs.<sup>5,7</sup> In this study, the impact of dose-dependent FVIII expression was tested in a model that has sustained FVIII transgene expression without underlying cellular damage or unwanted immune responses to the vector. This provides an opportunity to understand if the inherent differences in the FVIII synthesis in these approaches impact the cellular response. We sought to determine whether different levels of FVIII expression have local and systemic effects on the synthesis and secretion of FVIII, cellular stress, liver pathology and immune response to the protein.

## RESULTS

### Dose dependent expression of FVIII after AAV delivery

HA mice were administered AAV8-cFVIII using a SC delivery approach or TC delivery approach or AAV8-empty capsid (Figure 1a).<sup>5</sup> In the SC delivery approach the B-domain deleted cFVIII (cFVIII-BDD) is delivered as one transgene in an AAV vector and is synthesized as a single polypeptide chain closely mimicking the endogenous FVIII synthesis. The TC delivery approach codelivers the cFVIII heavy chain in one AAV vector and the cFVIII light chain in a second AAV vector. This approach takes advantage of the normal intracellular processing of FVIII that cleaves a single polypeptide into two chains forming a heterodimer. The FVIII heavy chain and FVIII light chain are synthesized as two separate polypeptide chains that come together to form a heterodimer, the secreted form of the protein. Earlier studies suggest that the chains must be coexpressed in the same cell to produce functional FVIII.<sup>5,19,20</sup> Our previous studies in both HA mice and HA dogs demonstrated that both approaches result in expression of therapeutic levels of functional FVIII.<sup>5</sup> Each delivery approach was administered at three AAV doses ( $1 \times 10^{10}$ ,  $5 \times 10^{10}$ ,  $2.5 \times 10^{11}$  vg/mouse). In the case of the TC delivery, this dose represents the total vector dose (e.g.,  $0.5 \times 10^{10}$  AAV8-FVIII-heavy chain vg/mouse and  $0.5 \times 10^{10}$  AAV8-FVIII-light chain vg/mouse). The AAV vector doses were selected to attain levels of FVIII at a range similar to the levels expressed in dogs (6–10%, low dose), in a normal range (50–100%,

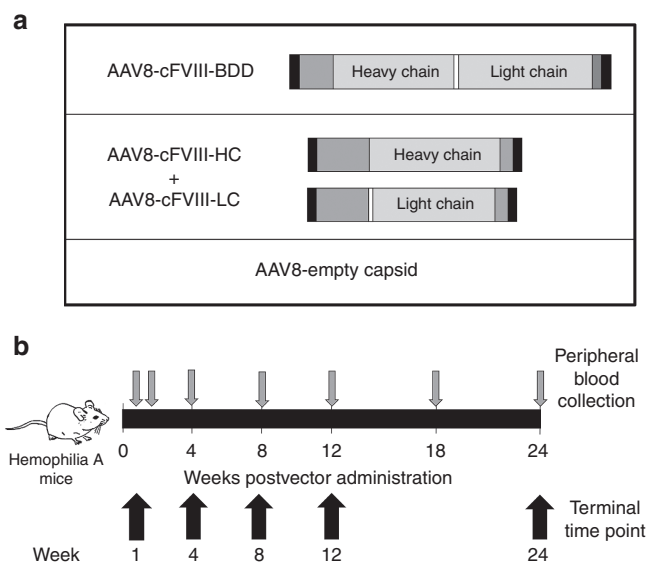


**Figure 1** Design of the AAV vectors and the experimental plan. (a) Factor VIII AAV vector constructs. AAV8 was used to deliver the wild type B-domain deleted (BDD) canine FVIII (cFVIII) as a SC (AAV8-hAAT-cFVIII-BDD) or to codeliver the heavy chain (HC) and the light chain (LC) in two separate AAV vectors (AAV8-TBG-cFVIII-HC and AAV8-TBG-cFVIII-LC). Empty capsids that did not contain a transgene were also delivered (AAV8-Empty capsid). (b) Experimental design. Each AAV vector was delivered to HA mice at three vector doses:  $1 \times 10^{10}$  vg/mouse ( $4 \times 10^{11}$  vg/kg) (low dose),  $5 \times 10^{10}$  vg/mouse ( $2 \times 10^{12}$  vg/kg) (mid dose), and  $2.5 \times 10^{11}$  vg/mouse ( $1 \times 10^{13}$  vg/kg) (high dose) ( $n = 3-5$  mice/cohort). At specific time points (1, 2, 4, 8, 12, 18, and 24 weeks) after AAV delivery, peripheral blood was collected (gray arrows). At the terminal time points (1, 4, 8, 12, or 24 weeks post vector administration) for liver harvest.

middle dose) and  $>100\%$  of normal (200–300%, high dose). At specific time points after vector administration (1, 2, 4, 8, 12, 18, and 24 weeks) peripheral blood was collected for analysis of FVIII antigen, cFVIII activity, anti-cFVIII antibodies as well as liver function tests (Figure 1b). Dose cohorts were assigned a terminal time point (1, 4, 8, 12, or 24 weeks post vector administration) for liver harvest.

At 2 weeks after vector administration, the antigen and activity reached peak expression levels (Figure 2) and by 4 weeks some animals had developed antibodies to the protein. Since these mice were immune competent HA mice, the immune response to cFVIII confounds the ability to accurately determine antigen and activity due to the neutralization and clearance of the protein. Thus, the levels at 2 weeks post vector administration provide the best assessment of the FVIII levels. At 2 weeks the circulating FVIII levels in the treated SC treated animals at the low, middle and high dose were  $10.6 \pm 3.9$ ,  $159.2 \pm 82.0$ , and  $431.5 \pm 183.8$  ng/ml, respectively (Figure 2a) and the activity was in agreement with the antigen levels. In the TC delivery treated animals, the levels of light chain in the circulation were twofold to fourfold higher than the heavy chain as we previously observed (Figure 2b).<sup>5</sup> At 2 weeks post vector administration these mice expressed  $8.0 \pm 2.6$  heavy chain and  $39.9 \pm 17.6$  light chain at the low dose;  $89.0 \pm 63.2$  heavy chain and  $132.0 \pm 52.5$  light chain at the middle dose; and  $149.6 \pm 98.6$  heavy chain and  $400.4 \pm 188.0$  ng/ml light chain at the highest dose. The FVIII activity in the TC treated mice correlated with the amount of heavy chain detected, as previously observed.<sup>5</sup>

Dose-dependent anti-FVIII antibody development in HA mice

The onset of anti-hFVIII antibody development was vector dose dependent (Figure 3). The anti-FVIII antibodies could be detected in some animals at 4 weeks postvector administration in mice that were treated at the highest vector dose. By 8 weeks post vector administration, additional animals in all dose cohorts had detectable IgG antibodies to FVIII. At that time point, 11% of the low dose ( $n = 15$ ), 40% of the middle dose ( $n = 10$ ), and 36% of the high dose ( $n = 11$ ) mice that had been treated with the SC vector had developed antibodies. In the TC approach, 8% of the low dose ( $n = 12$ ), 50% of the mid dose ( $n = 10$ ), and 91% of the high dose ( $n = 11$ ) animals

had developed antibodies to FVIII. However, over time the number of animals that had detectable anti-FVIII antibodies increased. By 18 weeks most of the mice (96%) that were followed to that time point ( $n = 26$ ) whether treated with the TC or SC approach had developed antibodies to FVIII. While the kinetics of antibody development was different among the delivery approaches, the outcome was identical with most of the mice developing anti-FVIII antibodies.

While there was significant variability in the IgG antibody titers, the titers were vector dose dependent. At the low dose of AAV, the mice had peak IgG titers ( $4\text{--}13\ \mu\text{g/ml}$ ) that was  $7.6\ \mu\text{g/ml} \pm 5.4$  for SC treated mice and  $6.5\ \mu\text{g/ml} \pm 5.7$  for TC treated mice. At the middle vector dose the titers were  $5\text{--}20\ \mu\text{g/ml}$  for both the SC ( $12.4\ \mu\text{g/ml} \pm 4.8$ ) and the TC treated mice ( $15.3\ \mu\text{g/ml} \pm 8.4$ ). The animals treated at the highest AAV dose had a wide range of antibody detected ( $17\text{--}60\ \mu\text{g/ml}$ ) ( $23.6\ \mu\text{g/ml} \pm 21.0$  SC;  $35.8\ \mu\text{g/ml} \pm 10.8$  TC).

A Bethesda assay was performed to determine if the antibodies that were detected in these animals were neutralizing antibodies (inhibitors). At the 18-week time point, all of the mice that had detectable IgG also had Bethesda titers that for the low dose cohorts were between 3.6 and 9.0 for TC treated animals which was similar to the SC treated animals (2.4–7.0 BU). However, the Bethesda titers for the high dose treated animals ranged from 3.3 to 70 BU.

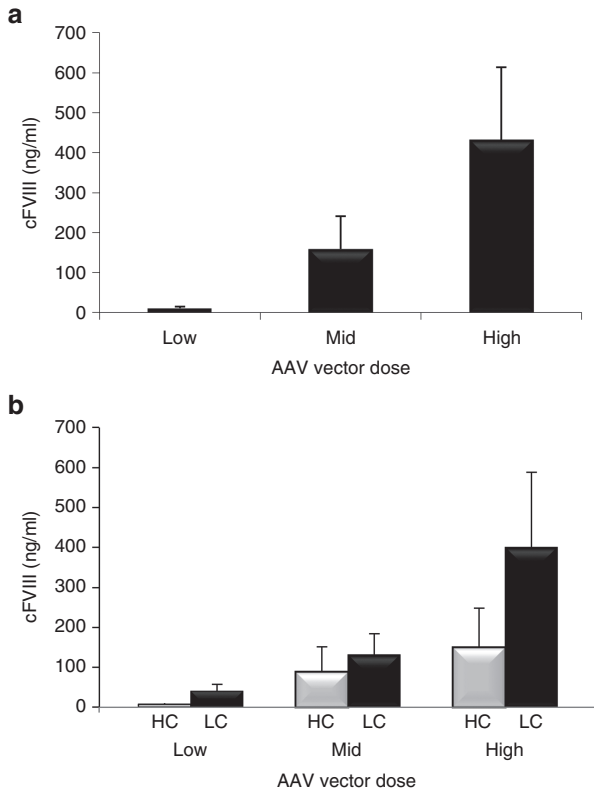


**Figure 2** FVIII expression after adeno-associated viral (AAV) delivery in hemophilia A (HA) mice. At 2 weeks post vector administration the canine FVIII (cFVIII) antigen levels were detected by enzyme-linked immunosorbent assay (ELISA). Three vector doses were analyzed:  $1 \times 10^{10}$  vg/mouse (low),  $5 \times 10^{10}$  vg/mouse (mid) and  $2.5 \times 10^{11}$  vg/mouse (high). (a) AAV8-canine FVIII (cFVIII)-BDD treated HA mice. (b) AAV8-cFVIII-HC and AAV8-cFVIII-LC treated HA mice. ELISA was used to detect the cFVIII-heavy chain (HC) and the cFVIII-light chain (LC) antigen levels.

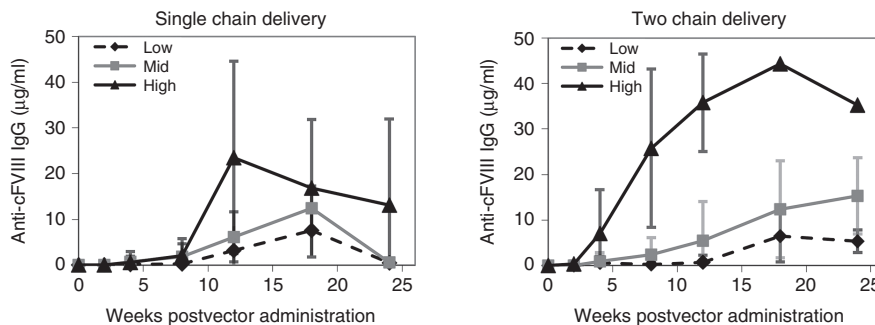


**Figure 3** Immune response to FVIII after AAV delivery. Anti-cFVIII IgG was determined after AAV delivery in AAV8-cFVIII-BDD treated HA mice (left panel) and AAV8-cFVIII-HC and AAV8-cFVIII-LC treated HA mice (right panel). AAV, adeno-associated viral; cFVIII, canine FVIII; HA, hemophilia A; HC, heavy chain; LC, light chain.

induces the UPR in this provocative setting as previously observed<sup>16</sup> and that there is no inherent difference between these two proteins in their ability to induce the UPR. The analysis was performed using the mean of the untreated HA controls ( $n = 3$ ) defined as 1.0. Tunicamycin treated HA mice controls ranged between 22-fold and 54-fold higher ( $39.3 \pm 16.2$ ) (BiP), and from 41-fold to 74-fold higher ( $62.0 \pm 18.2$ ) (CHOP) than the untreated animals.

At the low AAV vector dose ( $1 \times 10^{10}$  vg/mouse) (Figure 4a), small increases in BiP and CHOP mRNA were detected in the SC treated mice but also in the empty capsid treated cohorts. At 4 weeks post vector administration, BiP mRNA was increased with a mean of  $2.7$ -fold  $\pm 2.5$  above the HA controls in the SC treated group but this

was also observed in the empty capsid cohort with a mean  $9.1$ -fold  $\pm 8.5$ . CHOP mRNA was not increased in most of the treated cohorts except for a slight increase of 1.5-fold at the 1-week time point for the SC treated mice and the 4-week time point in the empty capsid treated mice (1.8-fold). No elevations in BiP or CHOP were observed in the mice that received the low dose of the TC delivery of FVIII.

At the middle AAV vector dose ( $5 \times 10^{10}$  vg/mouse), increases in BiP and CHOP transcripts were only observed in the SC treated cohorts. Increases in BiP expression of  $12.5$ -fold  $\pm 11.4$  and CHOP expression of  $2.0$ -fold  $\pm 1.6$  were observed at the 4-week time point in the SC treated mice (Figure 4b). Thus, modest transient increases in BiP and CHOP were observed in some mice that were treated with the SC

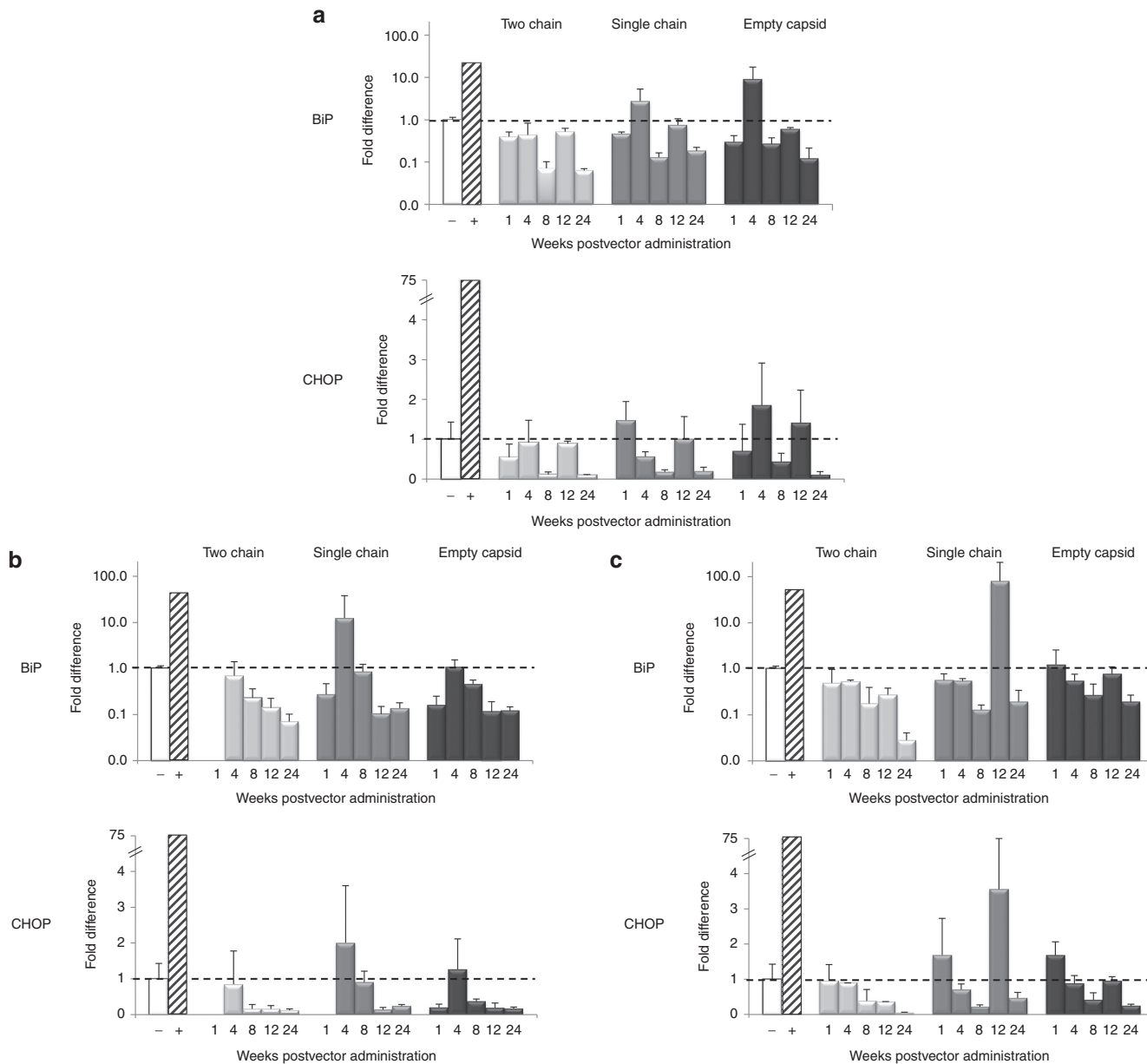


**Figure 4** Analysis of BiP and CHOP mRNA levels in the liver after AAV delivery. Quantitative PCR of BiP and CHOP mRNA levels was performed using RNA isolated from liver of the AAV-FVIII and the AAV-empty capsid treated mice at the terminal time points for each dose cohort. The HA mice ( $n = 3$ ) served as the negative control (–)(white bar) and tunicamycin treated mice were the positive control (+)(hatched bar). The two chain treated mice (light gray), SC treated mice (gray) and empty capsid treated mice (black) are shown at time points (1, 4, 8, 12, and 24 weeks) after AAV administration ( $n = 3$ –5 mice/cohort). (a) Low AAV dose ( $1 \times 10^{10}$  vg/mouse) treated HA mice. (b) HA mice treated at the middle AAV dose ( $5 \times 10^{10}$  vg/mouse). (c) High AAV dose ( $2.5 \times 10^{11}$  vg/mouse) treated HA mice. AAV, adeno-associated viral; BiP, binding immunoglobulin protein; CHOP, C/EBP homologous protein; HA, hemophilia A; PCR, polymerase chain reaction.



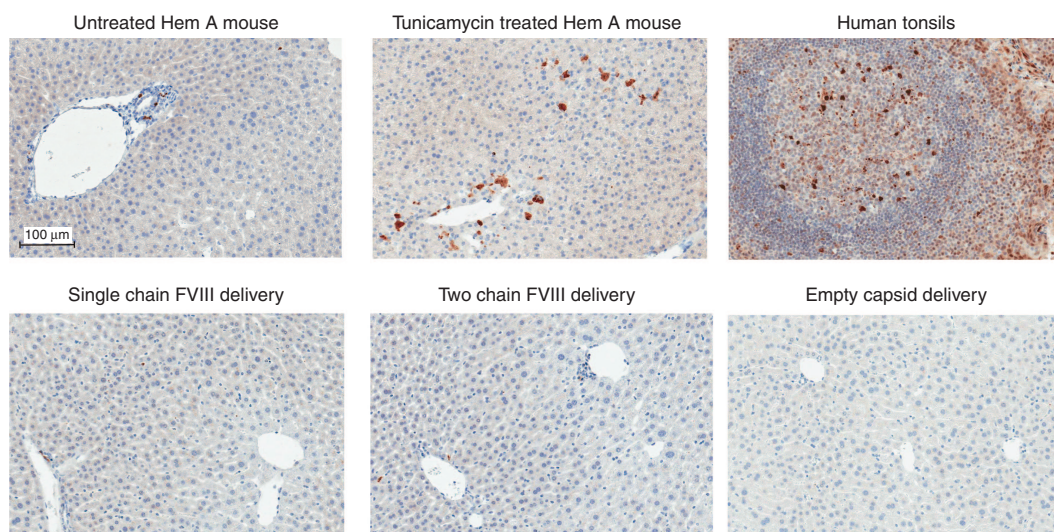


**Figure 5** Caspase 3 staining of liver to detect apoptosis. Caspase 3 staining was performed on paraffin embedded sections of liver tissue from multiple lobes of the liver. Tunicamycin treated mice and human tonsils served as positive controls while untreated hemophilia A (HA) mice were negative controls. These panels are representative of the sections that were analyzed for each cohort.

vector containing the B-domain deleted FVIII transgene. However, there was significant variability among the mice within these cohorts.

In the cohorts of mice receiving the highest vector dose ( $2.5 \times 10^{11}$  vg/mouse) (Figure 4c), only the SC treated HA mice had elevations in the BiP and CHOP markers. Modest increases in CHOP mRNA were detected at the 1-week time point in the SC (1.7-fold  $\pm$  0.7) and empty capsid (1.7-fold  $\pm$  0.6) treated mice but no increase in BiP mRNA was detected at this time point. However, at the 12-week time point in the SC treated mice, there were increases in both BiP and CHOP mRNA in three of the four mice. At this time point the BiP expression was 80.1-fold  $\pm$  63.3 and the CHOP expression was 3.6-fold  $\pm$  2.9 higher than the control HA mice. No increases in BiP and CHOP mRNA levels were detected in the TC or empty capsid treated mice.

Further studies were performed delivering a high dose ( $2.5 \times 10^{11}$  vg/mouse) of the SC vector compared with empty capsid to focus on time points surrounding the 12-week time point. At 10 weeks post vector administration, none of the mice treated with a high dose of the SC vector alongside the empty capsid had elevations in BiP and CHOP. Additional mice treated at the 12-week time point showed two of five mice treated with the SC (BiP 1.3-fold  $\pm$  0.6; CHOP 2.3-fold  $\pm$  1.3) and none of the empty capsid treated mice had elevations in BiP and CHOP expression. Thus, a total of 55% (five of nine) of the mice treated with the SC vector had evidence for induction of the UPR at the 12-week time point. At 14 weeks post vector administration, one of five SC treated mice (BiP 0.7-fold  $\pm$  0.5; CHOP 0.7-fold  $\pm$  0.5) and one of four empty capsid treated mice (BiP 1.6-fold  $\pm$  1.3; CHOP 1.6-fold  $\pm$  0.9) had elevations in BiP and CHOP. Notably, increases in BiP mRNA coincided with increases in CHOP expression.

Since inflammation signaling pathways are linked to the UPR, we evaluated whether the immune response to FVIII was associated with activation of the ER stress pathways. There was no correlation between the anti-FVIII antibody titers and the increases in BiP and CHOP expression (data not shown). However, there was a temporal association of the peak anti-FVIII antibody titers in the SC treated mice and the activation of the UPR. Overall, these results suggest that only transient induction of the UPR may occur at supraphysiological levels of FVIII expression after AAV SC delivery.

No evidence for apoptosis or altered liver function in AAV treated HA mice

Caspase 3 staining was performed on liver tissue from the terminal time points to determine if there was evidence for apoptosis in the AAV-FVIII treated mice compared with AAV-empty capsid treated mice (Figure 5). The tunicamycin treated animals had detectable caspase 3 staining. The AAV treated mice had a very low level of caspase 3 staining in the liver that was similar to the untreated HA mice. Terminal deoxynucleotidyl transferase (dUTP) nick-end labeling staining that detects DNA fragmentation that results from apoptotic signaling pathways was in agreement with the caspase 3 staining (data not shown). Thus, even in animals with increases in BiP and CHOP transcripts, no increase in apoptosis was detected after AAV delivery of FVIII. This is in contrast to the apoptosis that is detected after hydrodynamic delivery of FVIII (see Supplementary Figure 2).<sup>16</sup> Histologically, no differences were observed between the untreated and treated animals. Few small, scattered foci were associated with the central veins with no evidence of hepatocyte damage.

To determine if the liver enzymes may serve as a marker of cellular stress and to determine if the liver function was affected by the AAV vector dose, alanine aminotransferase (ALT) levels were assessed in the animals treated with the SC approach (Figure 6). Since the SC treated mice were the only mice to demonstrate evidence for the UPR, the ALT analysis focused on this group. No significant difference in the ALT levels between the cohorts was observed at any time point. At week 8 and 18 there was more variability in the ALT levels as shown by elevated levels in several mice. However, there was no correlation between elevations in BiP and CHOP mRNA and ALT levels. Thus, ALT did not serve as a marker of increased BiP and CHOP at the time points that were evaluated. Moreover, high level FVIII expression did not have an adverse effect on liver function.

## DISCUSSION

*In vivo* cellular stress may affect the efficacy and safety of FVIII expression. In the setting of gene transfer using any vector, the transgene copy number per cell is not regulated. Thus, there is significant heterogeneity in expression levels per cell. As gene delivery systems improve and increase transduction efficiencies, the gene copy per cell and thus the protein load per cell may further increase.

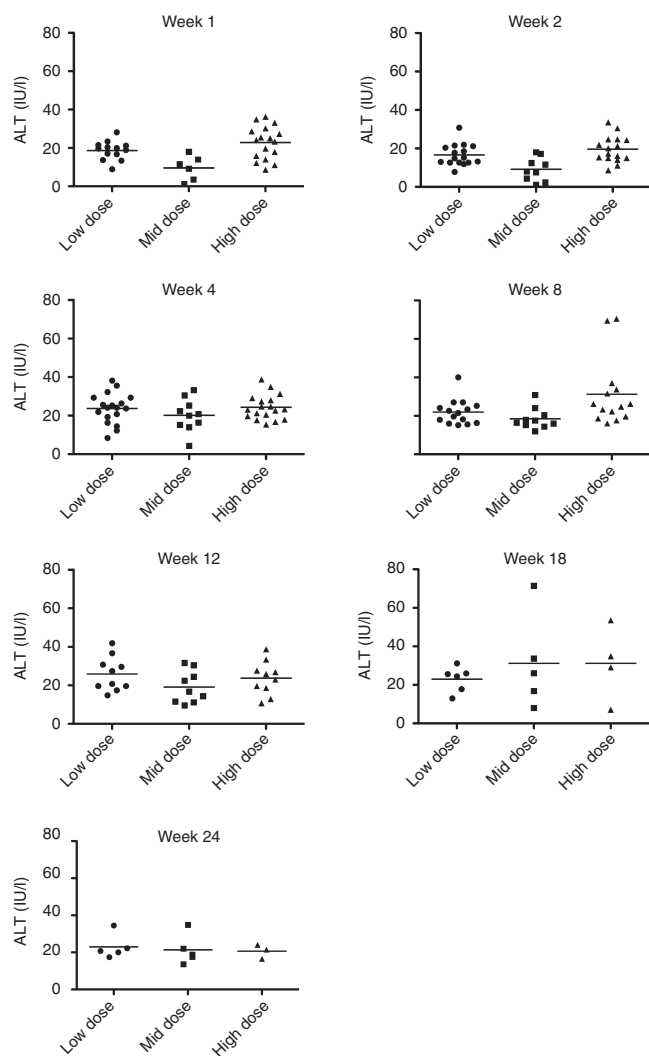


**Figure 6** Alanine aminotransferase (ALT) levels in the single chain (SC) treated animals. The ALT levels (IU/l) were determined for the hemophilia A (HA) mice treated at all three vector doses of the AAV8-cFVIII-BDD vector. Normal ALT levels for mice are in the range of 17–77 U/l. AAV, adeno-associated viral; cFVIII, canine FVIII.

For a secreted protein such as FVIII, the protein should not accumulate in the cell but it requires the cell to process and traffic a significant amount of protein through the ER/Golgi network. If the cell cannot adapt to the large protein load, the ER stress pathways are activated to allow the cell to adjust to the protein burden. However, prolonged ER stress may lead to apoptosis. After gene therapy, activation of these pathways could jeopardize the long-term expression of the transgene.

In this study, vector dose dependent induction of cellular stress responses was only observed in animals that expressed >200% of normal FVIII levels after delivery of the SC vector. Interestingly, mice that expressed similar high levels of FVIII after the TC delivery approach did not show evidence of the UPR suggesting that the large single FVIII polypeptide may be more prone to activate the cellular stress response. The individual polypeptide chains, the heavy chain and light chain, are each transported to the ER independently and may interact with protein chaperones within the ER in a different manner than the SC form. Thus, the individual chains may traffic through the ER and Golgi more efficiently than the SC form without inducing

the UPR. Even in the mice that demonstrated activation of BiP and CHOP, the response was transient and only detectable at a late time point. It should be noted that there was significant variability in the response with only about half of the mice at the 12-week time point showing evidence for the UPR. This variability may be due to variation in the protein expression per cell or to differences in the kinetics of this transient response that prevented detection of the UPR at the time points evaluated. Importantly, at AAV doses that resulted in <100% of normal FVIII levels, no activation of the UPR was observed. While the FVIII expression reached peak levels within 2 weeks after AAV administration, the UPR was not detected until 12 weeks post vector administration. The kinetics of the response supports that sustained high level FVIII expression may ultimately activate the UPR *in vivo*. CHOP is a proapoptotic transcription factor activated late in the UPR. While the increase in CHOP transcripts was detected at 12 weeks post AAV administration, there was no evidence for apoptosis in any of the AAV treated animals. Studies of AAV-hFVIII by Zolotukhin and colleagues (see companion paper, *Mol Ther Methods Clin Dev* 3, 16063, 2016) demonstrate that hFVIII also induces a transient cellular stress response after AAV delivery with no evidence for apoptosis. While these studies focused on hFVIII and cFVIII, it is conceivable that murine FVIII may result in an altered cellular stress response due to species-specific differences in these proteins that may affect interactions with the protein chaperones in the ER that could affect the UPR. Overall, transient activation of the ER stress response after AAV delivery of FVIII was not sufficient to lead to significant hepatocyte cell death.

In these studies, immunocompetent HA mice were used to understand if there were any correlations between the immune response to FVIII, high levels of expression and the cellular stress response. A dose-dependent anti-FVIII immune response was observed in these mice. The kinetics of this response is different than observed with factor IX. After AAV administration the immune response to FIX is detected in some mouse strains within 3–4 weeks<sup>22,23</sup> while the immune response to FVIII was not detected in some animals until after 10 weeks post vector administration. While there was a trend toward higher anti-FVIII antibody titers in the TC treated mice compared with the SC treated animals in the high dose cohorts, there was extensive variability in the antibody titers and all of the mice in these groups developed antibodies to FVIII. Dose-dependent immune responses to FVIII that develop after 8 weeks from vector administration in the HA mouse have been observed by other groups.<sup>6,24,25</sup> Other studies have not observed an immune response to FVIII suggesting differences in transgenes, levels of expression, study duration or mouse strains may impact the immune response.

Since the UPR is linked to inflammation pathways, it may be important to understand if high level FVIII expression is associated with cellular stress and the immune response to FVIII. No correlation was observed between the anti-AAV antibody titers and the increase in expression of BiP and CHOP. The animals that had increases in BiP and CHOP had anti-FVIII antibody titers that were lower than other animals in the study. However, it is interesting that both the peak anti-FVIII immune response and increase in BiP and CHOP were detected at 12 weeks post AAV administration. In addition, the immune responses to FVIII were observed in the animals treated with the TC delivery approach where no ER stress responses were observed further supporting that the immune responses are not associated with the UPR. Furthermore, there was no anti-FVIII immune response observed by Zolotukhin and colleagues (*Mol Ther Methods Clin Dev* 3, 16063, 2016) yet there was evidence of cellular stress responses.

Different approaches are currently in development to increase the FVIII expression that is required to achieve therapeutic expression

of FVIII at clinically relevant vector doses. With the use of codon-optimization that has been shown to improve FVIII expression,<sup>8,26</sup> it will be important to consider that this alters the protein load per cell and ultimately may impact the likelihood of the UPR. Variants of FVIII that increase secretion are in development and may provide a strategy for reducing the likelihood of a cellular stress response. While the mechanisms are not yet completely understood, some of these variants may modulate the interactions with protein chaperones in the ER/Golgi network to improve secretion.<sup>8,27,28</sup>

Recently, the site of FVIII synthesis was identified as the endothelial cell.<sup>29,30</sup> However, hepatocytes are a major target cell for FVIII synthesis in the setting of gene transfer. This raises the interesting question about how the site of protein synthesis may impact the secretion of the functional protein but also impact cellular stress pathways. With the development of therapeutic approaches for HA targeting multiple cell types including hematopoietic stem cells,<sup>5,31</sup> platelets,<sup>32–34</sup> blood-outgrowth endothelial cells,<sup>35</sup> liver sinusoidal endothelial cells<sup>36</sup> and hepatocytes,<sup>5,8,9,37</sup> it will be important to understand the cellular synthesis of FVIII in other cell types not only for the efficacy but for the safety of gene-based therapeutics. Studies of FVIII expression in platelets suggests that high FVIII expression may lead to apoptosis further demonstrating the importance of considering the FVIII expression per cell.<sup>38</sup>

In the setting of AAV-mediated delivery of cFVIII in HA dogs, long-term expression of cFVIII at <10% of normal levels has been followed without evidence for toxicity.<sup>5,7</sup> Recent studies in nonhuman primates resulted in expression of 15–100% without evidence of toxicity, however, some animals developed an anti-hFVIII immune response as expected with a nonspecies specific transgene.<sup>8</sup> While recently developed FVIII expression cassettes have significantly improved the FVIII expression levels per genome copy, the protein load per cell may exceed those observed in early HA dog studies. While the TC delivery approach had no evidence for the UPR, the SC FVIII constructs are the only approach currently being developed for clinical studies. Thus, the efficacy and safety of long-term expression of FVIII should be evaluated in large animals. With the initiation of the first clinical trial of AAV-mediated gene delivery of FVIII (NCT 02576795), it will be important to understand the potential impact of these responses in the clinical setting.

## MATERIALS AND METHODS

### Administration of AAV vectors

Male HA Exon 16 knockout mice<sup>39,40</sup> on a C57BL6/129 background (8–10 weeks of age) were administered AAV8-hAAT-cFVIII or AAV8-TBG-cFVIII-heavy chain and AAV8-TBG-cFVIII-light chain or AAV8 empty capsid using transgene constructs were previously described.<sup>5</sup> AAV vectors were administered in a volume of 200  $\mu$ l of phosphate buffered saline/5% sorbitol via tail vein injection. Plasma samples were collected in 3.8% sodium citrate (1:9 v/v) by tail sectioning. Control mice were treated with 3  $\mu$ g/g body weight of tunicamycin in 150 mmol/l dextrose administered intraperitoneally and liver was harvested 48 hours or 96 hours postinjection.<sup>21</sup> All animal procedures were approved by the Institutional Animal Care and Use Committees at the University of Pennsylvania and the Children's Hospital of Philadelphia, Philadelphia, PA.

### Hydrodynamic delivery

Plasmid (100  $\mu$ g) was delivered intravenously in the tail vein into 8-week old C57BL/6 mice (Jackson Laboratories, Bar Harbor, ME) in a volume of saline that was equivalent to the blood volume of the mouse based on weight (0.1 ml/g mouse). At 24 hours postinjection administration peripheral blood was collected in 3.8% sodium citrate (1:9 v/v) and the liver was harvested.

### Adeno-associated viral vector

Recombinant AAV vectors were produced by triple transfection and purified by CsCl gradient centrifugation as previously described. Vector titers

were obtained by silver staining and Taqman PCR (Applied Biosystems, Foster City, CA). The AAV vectors were generated at the Children's Hospital of Philadelphia Research Vector Core.

### Assays to detect factor VIII antigen, activity, and anti-FVIII antibodies

FVIII expression was assayed using a cFVIII specific enzyme-linked immunosorbent assay as previously described.<sup>5</sup> FVIII activity was measured using a Chromogenix Coatest SP4 FVIII (Diapharma, Lexington, MA). Anti-cFVIII antibodies were detected by cFVIII-specific total IgG antibodies by enzyme-linked immunosorbent assay or by Bethesda assay.<sup>5,41</sup>

### Quantitative RT-PCR for BiP and CHOP

RNA was isolated from the liver tissue using TRIzol (Invitrogen, Carlsbad, CA) and cDNA was synthesized using SuperScript III First-strand Synthesis System (Invitrogen). Utilizing SYBR Green Real-Time PCR (Applied Biosystems, Warrington, UK), messenger RNA levels encoding BIP and CHOP were quantitated against a standard of linearized pCR 2.1-TOPO plasmid containing the BIP or CHOP cDNA. Murine 18S ribosomal RNA was used as a control to normalize the RNA levels. The fold induction of mRNA levels of BiP and CHOP were relative to the untreated HA controls. The primers used were as follows: human BIP forward, 5'-CATGGTTCTCACTAAAATGAAAGG-3'; human BIP reverse, 5'-GCTGGTACAGTAACTG-3';<sup>21</sup> human CHOP forward, 5'-CTGCCTTTCACCTTGAGAC-3'; human CHOP reverse, 5'-CGTTTCTGGGATGAGATA-3';<sup>16</sup> murine 18S forward, 5'-CGCTTCTTACCTGGTTGAT-3' and murine 18S reverse, 5'-GAGCGACCAAGGACCATA-3'.<sup>16</sup>

### Caspase 3 staining

Caspase 3 antibody (AF835; R&D Systems, Minneapolis, MN) was used to stain formalin-fixed, paraffin-embedded tissue. Staining was performed on a Bond Max automated staining system (Leica Microsystems, Buffalo Grove, IL). The Bond Intense R staining kit (Leica Microsystems) was used. The standard protocol was followed with the exception of the primary antibody incubation which was extended to 1 hour at room temperature, Avidin Biotin Blocking was added (Vector Laboratories, Burlingame, CA) and a Peptide Blocking step was added (DAKO, Carpinteria, CA). Caspase 3 antibody was used at 1:1,000 dilutions, and antigen retrieval was performed with E2 retrieval solution (Leica Microsystems) for 20 minutes. Biotinylated goat anti-rabbit secondary (BA-1000; Vector Laboratories) was used at 1:200 dilution. After staining, slides were rinsed, dehydrated through a series of ascending concentrations of ethanol and xylene and then cover-slipped. Stained slides were then digitally scanned at 20 $\times$  magnification on an Aperio CS-O slide scanner (Leica Microsystems).

### Alanine aminotransferase

ALT levels were determined using the ALT (SGPT) Reagent Set (Colorimetric, Endpoint Method) (Teco Diagnostics, Anaheim, CA). Normal ALT values for mice are in the range of 17–77 U/l.

### Statistical analysis

The values are presented as mean  $\pm$  SD. Statistical significance between the control and experimental groups was determined with the Prism 5 version 5.0b software (GraphPad Software).

## CONFLICT OF INTEREST

D.E.S. receives research funding from Spark Therapeutics.

## ACKNOWLEDGMENTS

We thank Jesse Chen and Timothy Lee for their technical assistance. We also thank Shangzhen Zhou and the Research Vector Core at The Children's Hospital of Philadelphia for generating the AAV vectors. Daniel Martinez and the Pathology Core at The Children's Hospital of Philadelphia provided assistance with the caspase 3 staining. This work was supported by a Bayer Hemophilia Early Career Investigator Award (D. Sabatino) and a grant from the Eastern Pennsylvania Chapter of the National Hemophilia Foundation (D. Sabatino).



REFERENCES

1. Peyvandi, F, Garagiola, I and Young, G (2016). The past and future of haemophilia: diagnosis, treatments, and its complications. *Lancet* **388**: 187–197.
2. Nathwani, AC, Tuddenham, EG, Rangarajan, S, Rosales, C, McIntosh, J, Linch, DC et al. (2011). Adenovirus-associated virus vector-mediated gene transfer in hemophilia B. *N Engl J Med* **365**: 2357–2365.
3. Nathwani, AC, Reiss, UM, Tuddenham, EG, Rosales, C, Chowdhary, P, McIntosh, J et al. (2014). Long-term safety and efficacy of factor IX gene therapy in hemophilia B. *N Engl J Med* **371**: 1994–2004.
4. George, LA and Fogarty, PF (2016). Gene therapy for hemophilia: past, present and future. *Semin Hematol* **53**: 46–54.
5. Sabatino, DE, Lange, AM, Altynova, ES, Sarkar, R, Zhou, S, Merricks, EP et al. (2011). Efficacy and safety of long-term prophylaxis in severe hemophilia A dogs following liver gene therapy using AAV vectors. *Mol Ther* **19**: 442–449.
6. Brown, HC, Wright, JF, Zhou, S, Lytle, AM, Shields, JE, Spencer, HT et al. (2014). Bioengineered coagulation factor VIII enables long-term correction of murine hemophilia A following liver-directed adeno-associated viral vector delivery. *Mol Ther Methods Clin Dev* **1**: 14036.
7. Jiang, H, Lillcrap, D, Patarroyo-White, S, Liu, T, Qian, X, Scallan, CD et al. (2006). Multiyear therapeutic benefit of AAV serotypes 2, 6, and 8 delivering factor VIII to hemophilia A mice and dogs. *Blood* **108**: 107–115.
8. McIntosh, J, Lenting, PJ, Rosales, C, Lee, D, Rabbani, S, Raj, D et al. (2013). Therapeutic levels of FVIII following a single peripheral vein administration of rAAV vector encoding a novel human factor VIII variant. *Blood* **121**: 3335–3344.
9. Anguela, XM, Elkouby, L, Toso, R, DiPietro, M, Davidson, RJ, High, KA et al. (2015). Adeno-associated viral vector delivery of optimized human factor VIII achieves therapeutic factor VIII levels in non-human primates. *Blood* **126** (23): 199.
10. Pittman, DD, Alderman, EM, Tomkinson, KN, Wang, JH, Giles, AR and Kaufman, RJ (1993). Biochemical, immunological, and *in vivo* functional characterization of B-domain-deleted factor VIII. *Blood* **81**: 2925–2935.
11. Pipe, SW, Morris, JA, Shah, J and Kaufman, RJ (1998). Differential interaction of coagulation factor VIII and factor V with protein chaperones calnexin and calreticulin. *J Biol Chem* **273**: 8537–8544.
12. Kaufman, RJ, Pipe, SW, Tagliavacca, L, Swaroop, M and Moussalli, M (1997). Biosynthesis, assembly and secretion of coagulation factor VIII. *Blood Coagul Fibrinolysis* **8 Suppl 2**: S3–14.
13. Kaufman, RJ, Wasley, LC and Dorner, AJ (1988). Synthesis, processing, and secretion of recombinant human factor VIII expressed in mammalian cells. *J Biol Chem* **263**: 6352–6362.
14. Zhang, K and Kaufman, RJ (2008). From endoplasmic-reticulum stress to the inflammatory response. *Nature* **454**: 455–462.
15. Pittman, DD, Tomkinson, KN and Kaufman, RJ (1994). Post-translational requirements for functional factor V and factor VIII secretion in mammalian cells. *J Biol Chem* **269**: 17329–17337.
16. Malhotra, JD, Miao, H, Zhang, K, Wolfson, A, Pennathur, S, Pipe, SW et al. (2008). Antioxidants reduce endoplasmic reticulum stress and improve protein secretion. *Proc Natl Acad Sci USA* **105**: 18525–18530.
17. Brown, HC, Gangadharan, B and Doering, CB (2011). Enhanced biosynthesis of coagulation factor VIII through diminished engagement of the unfolded protein response. *J Biol Chem* **286**: 24451–24457.
18. Staber, JM, Pollpeter, MJ, Arensdorf, A, Sinn, PL, Rutkowski, DT and McCray, PB Jr (2014). piggyBac-mediated phenotypic correction of factor VIII deficiency. *Mol Ther Methods Clin Dev* **1**: 14042.
19. Scallan, CD, Liu, T, Parker, AE, Patarroyo-White, SL, Chen, H, Jiang, H et al. (2003). Phenotypic correction of a mouse model of hemophilia A using AAV2 vectors encoding the heavy and light chains of FVIII. *Blood* **102**: 3919–3926.
20. Wang, Q, Dong, B, Firman, J, Roberts, S, Moore, AR, Cao, W et al. (2014). Efficient production of dual recombinant adeno-associated viral vectors for factor VIII delivery. *Hum Gene Ther Methods* **25**: 261–268.
21. Zhang, K and Kaufman, RJ (2008). Identification and characterization of endoplasmic reticulum stress-induced apoptosis *in vivo*. *Methods Enzymol* **442**: 395–419.
22. Cao, O, Hoffman, BE, Moghimi, B, Nayak, S, Cooper, M, Zhou, S et al. (2009). Impact of the underlying mutation and the route of vector administration on immune responses to factor IX in gene therapy for hemophilia B. *Mol Ther* **17**: 1733–1742.
23. Fields, PA, Arruda, VR, Armstrong, E, Chu, K, Mingozzi, F, Hagstrom, JN et al. (2001). Risk and prevention of anti-factor IX formation in AAV-mediated gene transfer in the context of a large deletion of F9. *Mol Ther* **4**: 201–210.

24. Matsui, H, Shibata, M, Brown, B, Labelle, A, Hegadorn, C, Andrews, C et al. (2009). A murine model for induction of long-term immunologic tolerance to factor VIII does not require persistent detectable levels of plasma factor VIII and involves contributions from Foxp3+ T regulatory cells. *Blood* **114**: 677–685.
25. Mah, C, Sarkar, R, Zolotukhin, I, Schlessing, M, Xiao, X, Kazazian, HH et al. (2003). Dual vectors expressing murine factor VIII result in sustained correction of hemophilia A mice. *Hum Gene Ther* **14**: 143–152.
26. Ward, NJ, Buckley, SM, Waddington, SN, Vandendriessche, T, Chuah, MK, Nathwani, AC et al. (2011). Codon optimization of human factor VIII cDNAs leads to high-level expression. *Blood* **117**: 798–807.
27. Miao, HZ, Sirachainan, N, Palmer, L, Kucab, P, Cunningham, MA, Kaufman, RJ et al. (2004). Bioengineering of coagulation factor VIII for improved secretion. *Blood* **103**: 3412–3419.
28. Siner, JI, Iacobelli, NP, Sabatino, DE, Ivanciu, L, Zhou, S, Poncz, M et al. (2013). Minimal modification in the factor VIII B-domain sequence ameliorates the murine hemophilia A phenotype. *Blood* **121**: 4396–4403.
29. Everett, LA, Cleuren, AC, Khoriaty, RN and Ginsburg, D (2014). Murine coagulation factor VIII is synthesized in endothelial cells. *Blood* **123**: 3697–3705.
30. Fahs, SA, Hille, MT, Shi, Q, Weiler, H and Montgomery, RR (2014). A conditional knockout mouse model reveals endothelial cells as the principal and possibly exclusive source of plasma factor VIII. *Blood* **123**: 3706–3713.
31. Doering, CB, Denning, G, Dooriss, K, Gangadharan, B, Johnston, JM, Kerstann, KW et al. (2009). Directed engineering of a high-expression chimeric transgene as a strategy for gene therapy of hemophilia A. *Mol Ther* **17**: 1145–1154.
32. Du, LM, Nurden, P, Nurden, AT, Nichols, TC, Bellinger, DA, Jensen, ES et al. (2013). Platelet-targeted gene therapy with human factor VIII establishes haemostasis in dogs with haemophilia A. *Nat Commun* **4**: 2773.
33. Greene, TK, Wang, C, Hirsch, JD, Zhai, L, Gewirtz, J, Thornton, MA et al. (2010). *In vivo* efficacy of platelet-delivered, high specific activity factor VIII variants. *Blood* **116**: 6114–6122.
34. Schroeder, JA, Chen, Y, Fang, J, Wilcox, DA and Shi, Q (2014). *In vivo* enrichment of genetically manipulated platelets corrects the murine hemophilic phenotype and induces immune tolerance even using a low multiplicity of infection. *J Thromb Haemost* **12**: 1283–1293.
35. Ozelo, MC, Vidal, B, Brown, C, Notley, C, Hegadorn, C, Webster, S et al. (2014). Omental implantation of BOECs in hemophilia dogs results in circulating FVIII antigen and a complex immune response. *Blood* **123**: 4045–4053.
36. Zanolini, D, Merlin, F, Feola, M, Ranaldo, G, Amoruso, A, Gaidano, G et al. (2015). Extrahepatic sources of factor VIII potentially contribute to the coagulation cascade correcting the bleeding phenotype of mice with hemophilia A. *Haematologica* **100**: 881–892.
37. Finn, JD, Ozelo, MC, Sabatino, DE, Franck, HW, Merricks, EP, Crudele, JM et al. (2010). Eradication of neutralizing antibodies to factor VIII in canine hemophilia A after liver gene therapy. *Blood* **116**: 5842–5848.
38. Greene, TK, Lyde, RB, Bailey, SC, Lambert, MP, Zhai, L, Sabatino, DE et al. (2014). Apoptotic effects of platelet factor VIII on megakaryopoiesis: implications for a modified human FVIII for platelet-based gene therapy. *J Thromb Haemost* **12**: 2102–2112.
39. Bi, L, Sarkar, R, Naas, T, Lawler, AM, Pain, J, Shumaker, SL et al. (1996). Further characterization of factor VIII-deficient mice created by gene targeting: RNA and protein studies. *Blood* **88**: 3446–3450.
40. Bi, L, Lawler, AM, Antonarakis, SE, High, KA, Gearhart, JD and Kazazian, HH Jr (1995). Targeted disruption of the mouse factor VIII gene produces a model of haemophilia A. *Nat Genet* **10**: 119–121.
41. Herzog, RW, Mount, JD, Arruda, VR, High, KA and Lothrop, CD Jr (2001). Muscle-directed gene transfer and transient immune suppression result in sustained partial correction of canine hemophilia B caused by a null mutation. *Mol Ther* **4**: 192–200.



This work is licensed under a Creative Commons Attribution-NonCommercial-ShareAlike 4.0 International License. The images or other third party material in this article are included in the article's Creative Commons license, unless indicated otherwise in the credit line; if the material is not included under the Creative Commons license, users will need to obtain permission from the license holder to reproduce the material. To view a copy of this license, visit <http://creativecommons.org/licenses/by-nc-sa/4.0/>

© The Author(s) (2016)

Supplementary Information accompanies this paper on the *Molecular Therapy—Methods & Clinical Development* website (<http://www.nature.com/mtrm>)